Thermally-constrained fluid circulation and seismicity in the Lesser Antilles subduction zone

Kingsley Ezenwaka, Boris Marcaillou, Mireille Laigle, Frauke Klingelhoefer, Jean-Frédéric Lebrun, Michele Paulatto, Youssef Biari, Frédérique Rolandone, Francis Lucazeau, Arnauld Heuret, et al.

Thermally-constrained fluid circulation and seismicity in the Lesser Antilles Subduction Zone

Ezenwaka, K.[a], Marcaillou, B. [a], Laigle, M. [a], Klingelhoefer, F. [b], Lebrun, J.-F. [c], Paulatto, M. [d], Biari, Y. [a, e], Rolandone, F. [f], Lucazeau, F. [g], Heuret, A. [h], Pichot, T. [b, i], Bouquerel H. [g]

[a] Université Côte d'Azur, CNRS, Observatoire de la Côte d'Azur, IRD, Géoazur, Valbonne, France.

[b] Geo-Ocean, Univ Brest, CNRS, Ifremer, UMR6538, F-29280 Plouzane, France.

[c] Géosciences Montpellier, Université de Montpellier, CNRS, Université des Antilles, Pointe à Pitre, Guadeloupe (FWI), France.

[d] Imperial College London, Department of Earth Science and Engineering, Prince Consort Road, UK.

[e] Capgemini – Oil & Gas Centre of Excellence, Technopole Hélioparc Bâtiment Newton, 4 Rue Jules Ferry, 64000, Pau, France.

[f] Sorbonne Université, CNRS, Institut des Sciences de la Terre de Paris, ISTeP UMR 7193, Paris, France.

[g] Université de Paris, Institut de physique du globe de Paris, CNRS, Paris, France.

[h] Université de Guyane, Géosciences Montpellier (UMR 5243), Cayenne, 97300, France.

[i] Beicip-Franlab, 232 avenue Napoleon Bonaparte Rueil-Malmaison, Paris 92500, France.

Abstract

At subduction zones, fluid circulation and elevated pore pressure are key factors controlling the seismogenic behavior along the plate interface by reducing absolute fault strength, increasing the time return of high magnitude co-seismic rupture and favoring aseismic slip. The Lesser Antilles is an end-member subduction zone where the slow subduction of numerous trans-oceanic fracture zones and patches of pervasively fractured, hydrated and serpentinized exhumed mantle rocks increase the water input. Heat-flow variations measured in the trench and the forearc during the Antithesis 1 cruise reveal heat advection by fluid circulation and shed a new light onto the thermal control of seismicity location in the subduction zone.

In the Northern Lesser Antilles, heat-flow anomalies, negative in the trench and positive in the forearc, reveal a ventilated fluid circulation with downward percolation of cold fluids at the sediment-starved, pervasively fractured trench and upward discharge of warm fluids through the Tintamarre Fault Zone in the forearc. In contrast, in the Central Lesser Antilles, a positive heat-flow anomaly at the trench and the accretionary wedge is typical of an insulated fluid circulation where warm fluids invade the plate interface flowing updip from the subduction depths up to the trench.

The investigated margin segments correspond with a very low number of interplate thrust earthquakes, illustrating the frequent statement that fluids in subduction zones tend to reduce the interplate coupling, favor slow to aseismic slip behavior, and increase the time return of large seismic events. Moreover, the location of intraslab, and supraslab earthquakes at depth beneath the Central Lesser Antilles suggest a close relation to temperature-related dehydration reactions.

Keywords

Thermal modelling, Heat-flow, Lesser Antilles, Subduction zone, Seismogenic zone, Serpentinite dehydration reaction

1. Introduction

In subduction zones, complex temperature-fluid interactions control predominantly the seismogenic behavior of the megathrust, which hosts most of the large (Mw>7) to great (Mw>8) subduction earthquakes in the world. The temperature increases with depth and the transition from shallow stable (aseismic) to deeper stick-slip (seismogenic) behavior along the interplate contact depends on mechanical and chemical processes promoting gouge consolidation at temperature of 60-150°C (Moore & Saffer, 2001, Vrolijk, 1990). At greater depth, the onset of deep stable sliding for a "normal type" oceanic crust is generally associated with temperatures of 350-450°C (Tse & Rice, 1986) and/or the interaction of the interplate with the serpentinized mantle wedge of the upper plate (Hyndman et al., 1997). However, subduction of exhumed ultramafic rocks of slow-spreading oceanic crust and deep fluid circulation may affect thermally and mechanically this evolution of the interplate sliding behavior. Pore fluid overpressure possibly correlates with patches of low interseismic coupling (e.g. Moreno et al., 2014) and promotes aseismic creep, slow-slip and very-low frequency earthquakes (SSE and VLFE) rather than large co-seismic ruptures (Saffer & Wallace, 2015, and Kodaira et al., 2004). Moreover, fluid circulation at depth partly controls earthquake recurrence (Byerlee, 1993, Sibson, 2013, Saffer & Tobin, 2011).

Fluids enter subduction zones through different processes at work before the trench. These processes includes fluids trapped in the subduction channel sediments (e.g. Calahorrano et al., 2008), or hydrothermal flow in the oceanic upper crustal aquifer (e.g. Fisher & Becker, 2000), or trapped at greater depth in hydrous minerals down to the lithospheric mantle through different types of structure such as trans-oceanic fracture zones (Cooper et al., 2020), large-scale detachments at slow-spread oceanic ridges (Marcaillou et al., 2021), crustal-scale folded ridge (Kodaira et al., 2004), or outer rise slab-bending faults (e.g. Ranero et al., 2003). Circulating fluids advect heat which may drastically change the oceanic plate geotherm prior to subduction, modulate temperatures along the plate interface and change the heat flow at the surface and the margin thermal structure with respect to that estimated from the model of a conductively cooling plate (Kummer & Spinelli, 2008; Harris et al., 2010; Harris et al., 2017; Harris et al., 2020; Spinelli et al., 2018). The effect of hydrothermal fluids on thermal structure depends on the mode of circulation. Thick, continuous and undeformed sediments in the trench prevent fluid exchange between the ocean and the crust and favor insulated hydrothermal circulation (Harris et al., 2017). In this context, warm fluids flowing from subduction depth updip along the basement aquifer may generate heat-flow values higher than that predicted by conductive heat transfer models in the accretionary wedge and at the trench (e.g., Nankai ; Spinelli & Wang, 2008). In contrast, fractured oceanic crust with a thin

sediment cover in the trench, and/or a deeply fractured forearc crust favor fluid-driven heat advection to and/or from the ocean, generating the so-called ventilated hydrothermal circulation (Harris et al., 2017). As a result, downward percolation of cold fluids in the trench may generate significantly lower heat-flow values than that predicted by conductive heat transfer models (e.g., Costa Rica; Harris & Wang, 2002). Moreover, in a deeply and pervasively fractured forearc, fluid upward migration along fault planes and expulsion at the seafloor can generate elevated heat flow (Pecher et al., 2017). Hence, measured heat-flow values significantly different from those expected for conductive heat transfer provide indirect constraint on fluids circulation at depth.

The Lesser Antilles is an end-member subduction zone, which undergoes the subduction of a slow-spreading oceanic lithosphere, partly made of exhumed, hydrated, serpentinized peridotite patches within the slab crust (Paulatto et al., 2017), fractured with pervasive detachment faults (Marcaillou et al., 2021) and/or highly hydrated trans-oceanic fracture zones (Cooper et al., 2020). Moreover, the Lesser Antilles seismicity is heterogeneous, with along-strike variations in b-value (Schlaphorst et al., 2016) and isolated nests of thrust-faulting earthquakes (Hayes et al., 2013). This subduction zone is thus a promising study area to investigate the influence of along-strike variations in deep hydrothermal circulation onto the interplate seismic activity. During cruises Antithesis 1 and 3, we acquired a grid of multichannel seismic (MCS), four trench-normal Wide-Angle Seismic (WAS) profiles, and heat-flow measurements along two trench-normal profiles at the Lesser Antilles Subduction zone (Marcaillou & Klingelhoefer, 2013a, 2013b, 2016). These measurements offshore of Martinique and Saint Martin islands respectively (Figure 1) aim at investigating heat-flow variations related to fluid circulation at depth. Drastic mismatches between measurements of heat flow and predictions assuming conductive cooling highlight the strong influence of fluid-driven heat advection on the heat-flow at the surface. We analyze pathways for fluid charge and discharge, the impact of this hydrothermal circulation on the regional heat-flow and the temperature along the interplate contact, and discuss the relation to the seismicity location in the Lesser Antilles Subduction Zone (LASZ).

2. Regional setting

2.1 Geodynamical and structural background

The Caribbean plate overthrusts the North and South American Plates in a N76° direction with a 2 cm/yr convergence rate (DeMets et al, 2000). In the study area, the calculated age of the subducting oceanic plate at the trench from the nearby magnetic anomaly C34 of the North American Plate ranges from 83 Ma east of Barbuda island to 98 Ma east of southern Martinique island (Carpentier et al., 2008). A dense geophysical dataset - including bathymetric, multichannel seismic and wide-angle seismic data - constrain the along-strike variations in structure of the LASZ (Kopp et al., 2011, Pichot et al., 2012, Laigle et al., 2013b, Evain et al., 2013, Paulatto et al., 2017, Laurencin et al., 2017, 2018, 2019, and Boucard et al., 2021).

The nature and structure of the Atlantic subducting crust is expected to vary both in the north-south and east-west directions. At slow-spreading mid-ocean ridges, magmatically-robust segments promote typical layer 2/3 "Penrose" structure (e.g. White et al., 1992), while tectonically-dominated segments generate stretched and thinned crust frequently hosting large bodies of exhumed, hydrated and serpentinized upper mantle peridotites (e.g. Cannat et al., 2006, Escartín et al., 2008). Numerous occurrences of tectonically-dominated basement have been observed near the Mid-Atlantic Ridge, where Oceanic Core-Complexes and Megamullions outcrop (e.g. Tucholke et al., 1998, Ildefonse et al., 2007, Szitkar et al., 2019), between the Mid-Atlantic Ridge and the Lesser Antilles Subduction Zone about 300 km from the trench (Davy et al., 2020), and at the Jacksonville Patch in the trench offshore of Barbuda island (Marcaillou et al., 2021). Moreover, numerous trans-oceanic fracture zones deeply hydrate the oceanic crust and mantle. The subducting Vema, Marathon, Mercurius and Doldrums Fracture zones of the South American Plate generate vigorous dewatering beneath the Central Lesser Antilles Arc (Cooper et al., 2020). The 15-20 Fracture Zone in the North American Plate (Braszus et al., 2021) located beneath the Northern Lesser Antilles forearc is likely to favor fluids circulation at depth (Marcaillou et al., 2021).

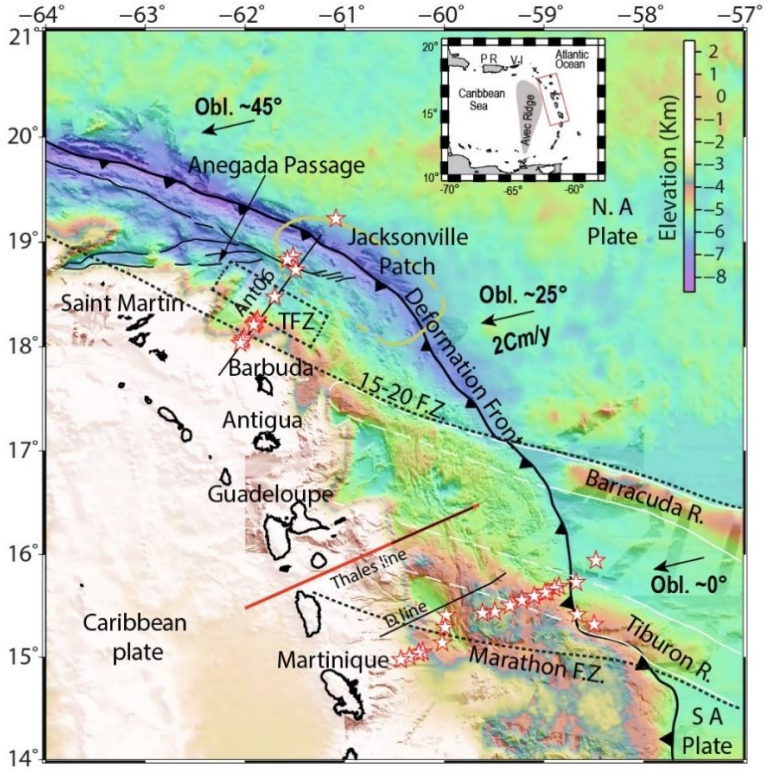

Figure 1: Bathymetric map of the Northern Lesser Antilles based on data recorded during cruises Antithesis I, III (Marcaillou & Klingelhoefer, 2013a, 2013b, 2016), Sismantilles II (Laigle et al., 2013a, b). The map shows the location for heat-flow measurements recorded during Antithesis cruise (plain stars), Multichannel and Wide-Angle seismic lines (black and red lines respectively) Ant06 (Laurencin et al., 2017, Boucard et al., 2021), Thales line (Kopp et al., 2011), D line (Laigle et al., 2013a, b). The black dotted line shows the projection onto the seafloor of the 15-20 and Marathon Fracture Zones, which deeply incise the subducting oceanic plate, and the dotted frame shows the 60-km-wide Tintamarre Fault Zone (TFZ) in the forearc. N A – North American, S A – South American, PR – Puerto Rico, VI – Virgin Islands.

The sediment thickness in the trench decreases northward from approximately ~3 km south of Tiburon Rise (Pichot et al., 2012) offshore of Martinique, to ~0.5 km north of Barracuda Ridge offshore of Saint Martin (Laurencin et al., 2019). The width of the accretionary prism also decreases from 110 to 30 km (Laurencin et al., 2019, Laigle et al., 2013b). Seismic lines in the Northern Lesser Antilles (Laurencin et al., 2017, Boucard et al., 2021) and in the Central Lesser Antilles (De Min et al., 2015, Laigle et al., 2013a, 2013b) show that the overall thickness of the forearc sedimentary layer and the margin basement is similar along-strike. In the forearc domain offshore of Antigua-Barbuda, the >100-km-long and 60-km-wide N120° trending Tintamarre Fault Zone deeply and pervasively fractures the margin (Figure 1) (Boucard et al., 2021). The slab dip angle shows apparent along-strike variation at the shallower part, when observed as a function of the distance from the trench. For instance, the slab dip is ~10° at 30 km and 110 km distance offshore of Saint Martin and Martinique islands respectively (Laurencin et al., 2019, Boucard et al., 2021, Kopp et al., 2011, Laigle et al., 2013b). This difference corresponds to the along-strike variation in accretionary wedge size. In contrast, the landward increase in slab dip angle is similar on the two profiles when observed as a function of interplate depth. At large depth, the slab dip angle is up to 51° at 280 km distance from the trench and shows no significant along-strike variation up to Guadaloupe (Paulatto et al., 2017), and Saint Martin when projected from Wide angle model of Klingelhoefer et al., (2018). The mantle wedge of the upper plate intersects the slab at 24 km and 28 km depth (~100 km and ~160 km from the deformation front) offshore of Saint Martin and Martinique islands respectively (Laurencin et al., 2018, Kopp et al., 2011).

2.2 Seismicity and seismogenic zone

A recent re-interpretation of the available campaign and continuous GPS measurements in the Caribbean resulted in a re-evaluated plate velocity field (van Rijsingen et al., 2021). These authors propose that the plate coupling along the Puerto-Rico and Lesser Antilles subduction interface is very low. Consistently, the seismicity catalogue record only a few hundred earthquakes per year in the Lesser Antilles (Figure 2). However, investigations on some coral micro-atolls suggest that vertical deformation are possibly related to a local increase in interseismic coupling at great depth (Philibosian et al., 2022). A more recent study (van Rijsingen et al., 2022) has however, presented vertical velocities for the Lesser Antilles Islands and examine the link between the short and long-term vertical motions and their underlying processes. Based on their elastic dislocation models, they show that a locked or partially locked interplate up to 60 km depth would produce uplift of the island arcs, which is opposite to the observations of microatolls and GNSS data. Thus, suggesting low coupling for this subduction zone.

During the historical period, only few earthquakes among damaging events occurred on the plate interface, including the largest 1843 event with an intensity-based magnitude possibly ranging between 7.0 (Bernard & Lambert, 1988) and 8.4 (Feuillet et al., 2011; Hough, 2013). The CMT catalog (Dziewonski et al., 1981; Ekström et al., 2012) indicate that only about 46 earthquakes along ~800-km-

long segment, with Mw > 5 and focal mechanisms consistent with a co-seismic rupture along the subduction interface, have been recorded teleseismically since 1973 (Figure 2). This scarce interplate seismicity is mainly aggregated in two clusters: one from Montserrat to Barbuda and the other from the Anegada Passage to the Virgin Islands. Between these regions and to the south of Guadeloupe, subduction earthquakes are very rare in the instrumental period, and small earthquakes (Mw < 5) dominate (Schlaphorst et al., 2016). The scarcity of subduction earthquakes raises the question of seismic gaps in the Lesser Antilles, particularly between Barbuda and the Anegada Passage (Marcaillou et al., 2021).

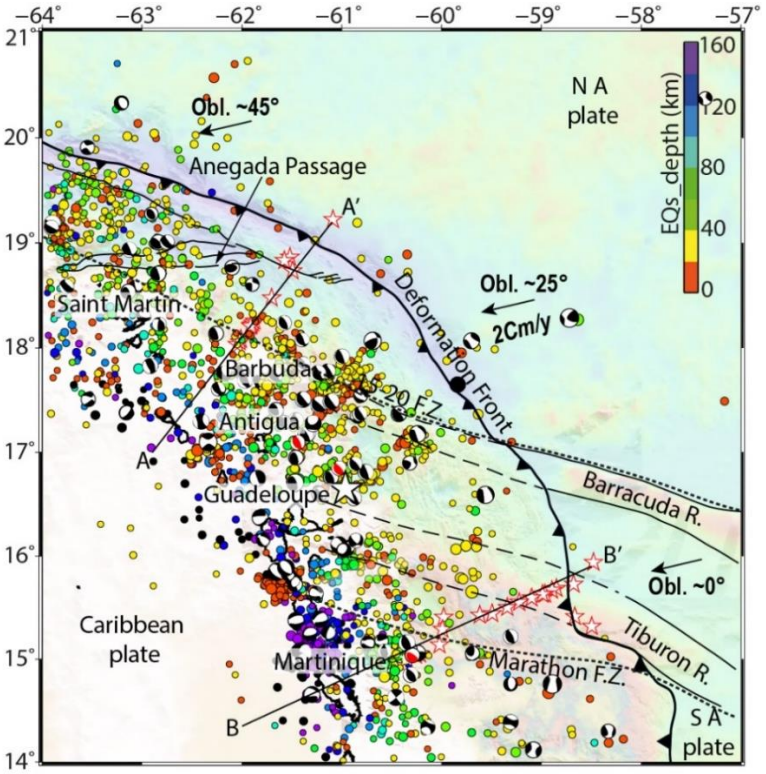

Figure 2: Seismicity distribution along the Lesser Antilles margin. The colored circles are the earthquakes from the USGS catalogue (Mw > 3.5 from 1900 to 2022), with size and color representing magnitude and epicentral depth, respectively. The black star represents the epicenter of the 1843 earthquakes. Black focal mechanisms are thrust-type earthquakes recorded teleseismically (from the gCMT catalogue 1976 – 2021). Red focal mechanisms are relocated flat thrust earthquakes based on OBS deployment (Laigle et al., 2013a). Black lines AA' and BB' show the location of the thermal models and the earthquake profiles shown in Figure 8.

2.3 Thermal regime

Prior to the Antithesis cruises, old, scarce and highly scattered heat-flow measurements existed in the Lesser Antilles forearc and the trench. More recent data were acquired in the Grenada backarc basin and Island arcs (Manga et al., 2012). Gutscher et al. (2013) proposed first thermal models at various latitudes along the Lesser Antilles. In their study, lines AA' and CC' approximately correspond to the Saint Martin and Martinique heat-flow profiles in the current study. However, along these two lines, the modelling resulted in a poorly constrained thermal structure. Offshore of Antigua, only one heat-flow

measurement (82 mW/m²) in the forearc constrain the model, and offshore of Martinique, old heat flow measurements scattered between 30 and 90 mW/m². Thus, the margin thermal structure needs to be re-evaluated in the Northern and Central Lesser Antilles.

3 Methods

During the Antithesis 1 cruise (Dec 2013 - Jan 2014), we acquired 39 heat-flow measurements using a microprocessor-controlled heat-flow (MCHF) instrument (see the Supplementary Material for description). We model the thermal structure of the subduction zone along two trench-normal profiles, one located between Barbuda and Saint Martin islands and crossing the volcanic arc at St Kitts island (hereafter named 'Saint Martin' profile), and the other crossing Martinique island forearc and active volcanic arc (hereafter named 'Martinique' profile) (Figure 1). The 2-D finite-element steady-state modelling method (Wang et al., 1997), the mesh geometry (Figure 3), the input parameters and the thermal boundary conditions are described in details in the supplementary material.

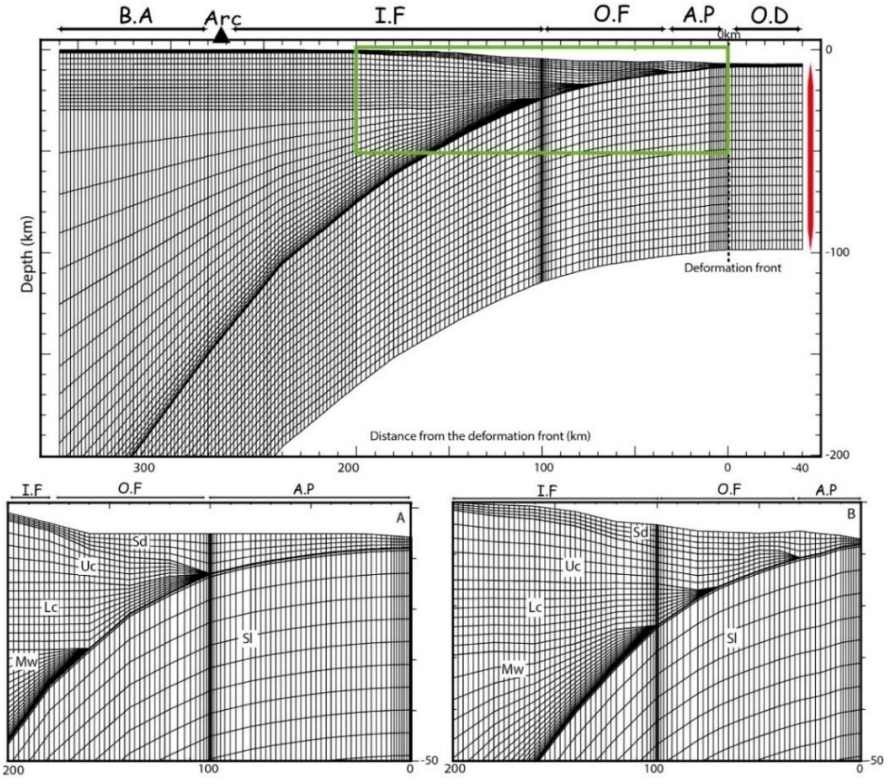

Figure 3 : Geometry of the finite element mesh used for the 2D steady-state thermal modelling. The green frame indicates projected regions for (A) Martinique profile and (B) Saint Martin profile. The red line indicates the location of the calculated oceanic geotherm. [O.D – Oceanic domain, A.P – Accretionary prism, O.F – Outer forearc, I.N – Inner forearc, B.A – Backarc, Sd – Sediment, Sl – Slab, Uc – Upper crust, Lc – Lower crust, Mw – Mantle wedge]

For conductive models, the geotherm at the oceanic boundary is calculated using a model of a conductive half-space cooling lithosphere based on a 1-D approach (Hutchison, 1985) and detailed by Marcaillou et al., (2008). However, fluid circulation within the incoming oceanic crust can cause

hydrothermal warming (e.g. Spinelli & Wang, 2008) or cooling (e.g. Harris & Wang, 2002) in the trench, and modify the heat flow at the surface, the oceanic geotherm and the temperature along the subduction interface. We use the methods by (Spinelli & Wang, 2008, Harris & Wang, 2002) to calculate the oceanic geotherm where anomalous heat flow (i.e. heat-flow different from conductive value) indicate significant heat advection. This approach requires the use of Nusselt number (Nu) as a proxy to model heat advection due to hydrothermal circulation (See the Supplementary material).

4 Regional heat-flow and fluid-driven heat advection

In the following, we describe the measured and calculated heat-flow values based on conductively cooling modelling and heat advection in order to discuss the influence of fluid circulation.

4.1 Measurements

We recorded 13 and 26 heat-flow measurements, at depth greater than 2400m, from 30-50 km before the trench up to the inner forearc, at the latitude of Saint Martin and Martinique respectively (Figure 1). Water depths for heat-flow measurements are indicated in Figure 4. Along the Martinique profile, the heat flow decreases progressively from ~78mW/m² in the trench to 35-45mW/m² at 100-150 km from the deformation front in the outer forearc and increases to ~60mW/m² towards the arc (Figure 4A). In contrast, along the Saint Martin profile, the heat flow does not significantly vary from the trench, ~42mW/m², to the forearc, where values range from 30 to 42mW/m² between 45 and 120 km from the deformation front (Figure 4B). The two profiles differ in two key ways. First, the heat flow is 53% higher in the trench offshore of Martinique than of Saint Martin. Moreover, the heat flow decreases from the trench to the outer forearc along the former but remains constant along the latter.

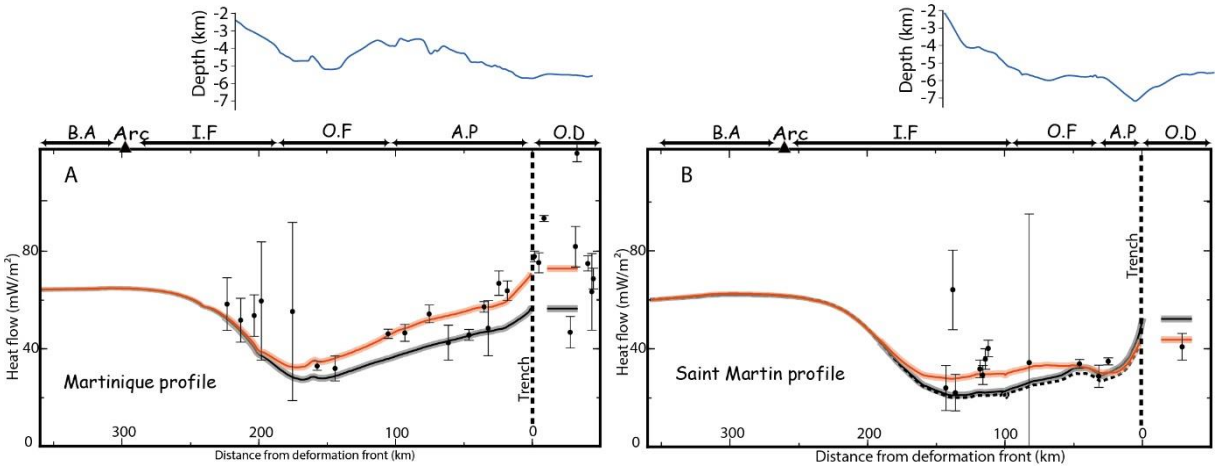

Figure 4: Measured and calculated heat-flow along Martinique profile (A) and Saint Martin profile (B). The figures show the heat-flow measurements (black dots), the calculated heat-flow for conductive models (black line) and for models including fluid thermal convection (red line) with 10% uncertainty (shaded area). In the oceanic domain, the horizontal lines are 1D calculated values. The dash line represent model without fluid expulsion in the forearc. The blue lines are the shapes of the bathymetry along the collected heat-flow data for the both profiles. [O.D – Oceanic domain, A.P – Accretionary prism, O.F – Outer forearc, I.N – Inner forearc, B.A – Backarc]

4.2 Calculated conductive heat flow

Conductive thermal modelling predicts a heat flow profile which decreases from the oceanic domain to the forearc, from 56 to 26 mW/m² along the Martinique Profile and from 52 to 22 mW/m² along the Saint Martin Profile (black lines in Figure 4A and Figure 4B). The calculated heat flow at the trench is consistent with the expected value for an 80-Myr-old oceanic plate (Stein & Stein, 1994; Lucazeau, 2019). Along both profiles, the calculated conductive heat flow poorly fits the measurements. Offshore of Martinique, the calculated heat flow is ~30% lower than the measurements in the trench and decreases westward similarly as the measurements, thus remaining significantly lower along the outer forearc. In other words, the heat-flow mismatch at the trench and the accretionary prism indicates a positive thermal anomaly compared to the conductive model at the margin front. In contrast, on Saint Martin profile, the calculated conductive heat-flow is ~23% higher than the measurement in the oceanic Jacksonville Patch (Figure 1). Moreover, the calculated heat-flow decreases westward, along the forearc and is lower than the measurements between 60 and 140 km from the deformation front. Thus, compared to the conductive model, this result indicates contrasting thermal anomalies: one negative near the trench and at the accretionary prism, the other positive at the forearc.

4.3 Sensitivity tests for the calculated conductive heat-flow

We performed sensitivity tests for the key-parameters of the conductively cooling model to check whether heat conduction can possibly account for the measured heat-flow variations, or if these variations are necessarily related to fluid-driven thermal advection.

In the frame of a conductively cooling oceanic lithosphere, the northward decrease in measured heat-flow from 78 to 42mW/m² in the trench is possibly related to two parameters: the incoming plate age and the oceanic sedimentation rate (Hyndman & Wang, 1993; Marcaillou et al., 2008). However, this decrease would require an increase in the oceanic plate age from 40 Myr to >120 Myr, which is highly unreasonable at the Lesser Antilles, where the age of the ~80-Myr-old American Plate does not vary significantly along-strike (Müller et al., 2019). Moreover, a sedimentation rate in the trench, offshore of Saint Martin, high enough to reduce the heat-flow by 23% is inconsistent with the <500-m-thick trench fill (Laurencin et al., 2019). Offshore of Martinique, the trench fill is up to 3 km thick (Pichot et al., 2012), but even a theoretical model with zero sedimentation rate results in calculated heat-flow that remains ~30% lower than the measurements. As a result, in the trench, heat conduction cannot generate the high heat-flow along the Martinique profile and low heat-flow along the Saint Martin profile without a key-contribution by heat advection.

Along the Saint Martin profile, measurements indicate an intriguingly stable heat-flow from the trench to the inner forearc, while typically at subduction zone, the heat-flow decreases as the oceanic plate deepens beneath the margin (Wang et al., 1995). In the conductively cooling model, the slab-dipping angle and the upper plate thermal conductivity are the key parameters that control the landward

decrease of the calculated heat-flow (Figure 4). Fitting the measurements by varying the slab-dipping angle is obtained when involving flat slabs geometries in the models (slab dip angle < 2°). However, offshore of Saint Martin, wide-angle models (Laurencin et al., 2018) and MCS data (Laurencin et al., 2019) show that the slab dip is up to ~25° beneath the forearc. In addition, fitting the measurements by varying the thermal conductivity in the upper-plate and the sediments would require values greater than 10 $W.m^{-1}.K^{-1}$, which is unrealistic for these lithologies (Beardsmore & Cull, 2010).

These tests thus indicate that conductively cooling models cannot satisfactorily account for 1) the heat-flow in the trench, which is too high offshore of Martinique and too low offshore of Saint Martin and 2) the high heat-flow at 60-140 km from the deformation front at the forearc of Saint Martin.

4.4 Calculated heat advection

Offshore of Martinique, anomalously high heat flow in the trench and at the deformation front is typical of the hydrothermal warming related to insulated circulation: warm fluids flow updip along the oceanic basement aquifer to the trench, where thick and poorly faulted sedimentary fill reduces exchanges with seawater (Spinelli & Wang, 2008, Harris et al., 2010). A similar insulated system has been observed and modelled in the Nankai subduction zone (Spinelli & Wang, 2008). We applied the methodological approach used by these authors to model heat advection (See the Supplementary material). In this approach, increasing the Nusselt Number (Nu) in a mesh layer that represent the crustal aquifer simulates fluid flow along this region. Using Nu of 1000, consistent with previous modelling in other subduction zones (e.g. Harris et al., 2020), results in higher calculated heat-flow of 76mW/m² in the trench and at the deformation front, which is consistent with the measurements. The addition of fluid advection results in a landward decreasing calculated heat-flow that fits the measurements from the trench to the inner forearc (red line in Figure 4A).

Offshore of Saint Martin, anomalously low heat-flow in the poorly sedimented and pervasively fractured trench is typical of ventilated hydrothermal systems where cold seawater percolates through oceanic basement faults (e.g. Harris & Wang, 2002). In Costa-Rica, these authors successfully modelled hydrothermal cooling by reducing the oceanic geotherm of the incoming plate. In our model, reducing the oceanic geotherm at the seaward boundary results in lowering the calculated heat-flow to 45 mW/m², in the trench and at the margin deformation front (black dotted line in Figure 4B) which is consistent with the measurements. Hydrothermal cooling in the trench reduces the calculated heat-flow along the accretionary wedge where it fits the measurements, but does not significantly change the calculated value beneath the forearc (60-140 km from the deformation front) where it remains much lower than the measurements. This positive thermal anomaly in the forearc corresponds to the location of the Tintamarre Fault Zone suggesting warm fluid upward migration to the seafloor as consistently proposed by previous studies based on tectonic observations (Boucard et al., 2021), wide-angle derived velocity anomaly (Klingelhoefer et al., 2018) and discussion from geochemical data (Cooper et al., 2020). We model this heat migration, using a Nusselt Number of 3.5 at the forearc area where the Tintamarre Fault

Zone (TFZ) deeply fracture the margin (Figure 5). The TFZ covers ~100 km wide and ~6km depth (second layer in the close up in Figure 5B), and is in line with the extent of the faults zone as imaged in seismic and bathymetric data (Boucard et al., 2021). This value of Nu accounts for the thermal effects of heat transfer by fluid circulation in this unit. This modelling generates heat-flow of 34 mW/m² at the surface, which fits the measurements (Figure 4b) and thus approximate the upward heat migration in the Tintamarre Fault Zone.

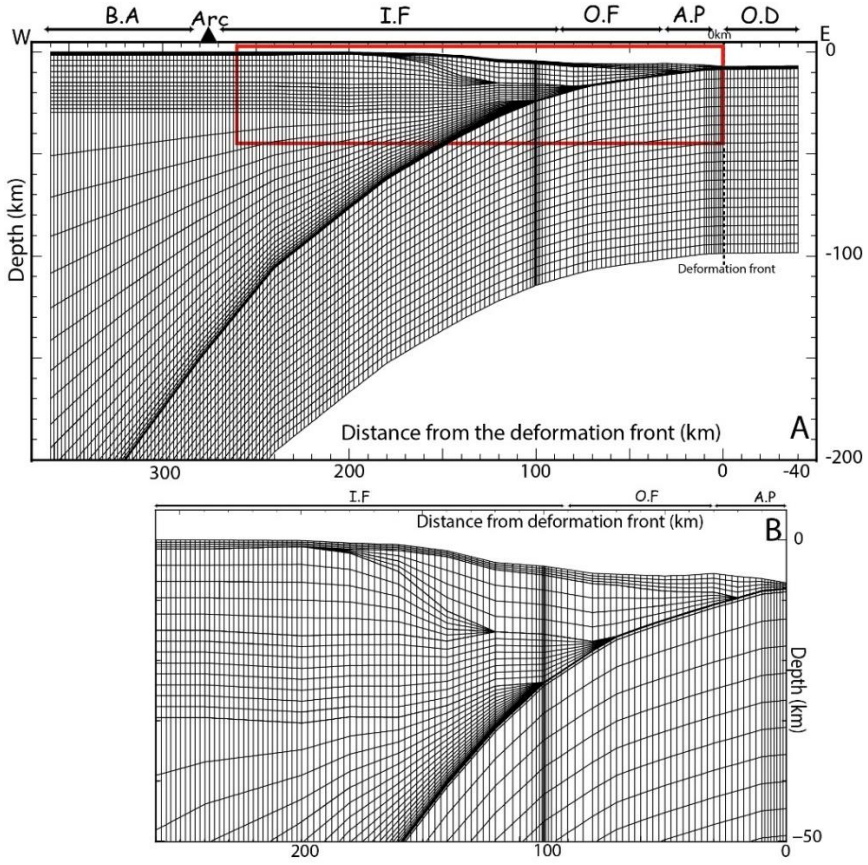

Figure 5: Global view (A) and close up (B) of the modified 2D mesh grid for the Saint Martin. The mesh includes a theoretical layer, which corresponds with the forearc area where the Tintamarre Fault Zone deeply and pervasively fractures the margin. Increasing the Nusselt Number in this layer (see supplementary material) accounts for the high heat-flow measured in surface, inconsistent with conductive modelling and thus likely related with upward fluid-driven heat-flow along the Tintamarre Fault planes.

5 Hydrothermal circulation within the Lesser Antilles subduction zone

Measurements provide unexpected heat-flow values in the trench, at the deformation front and in the forearc of the Lesser Antilles Subduction Zone. Conductively cooling modelling cannot predict heat-flow values which satisfactorily fit the measurements indicating that fluid-driven heat advection strongly influences the heat transfer in the margin segments. This result is consistent with an increasing number of recent studies, which conclude that the LASZ is extremely hydrated (e.g. Schlaphorst et al., 2016, Paulatto et al., 2017, Cooper et al., 2020, Marcaillou et al., 2021). Moreover, the measurements and models indicate that the fluid circulation varies along-strike, as discussed below.

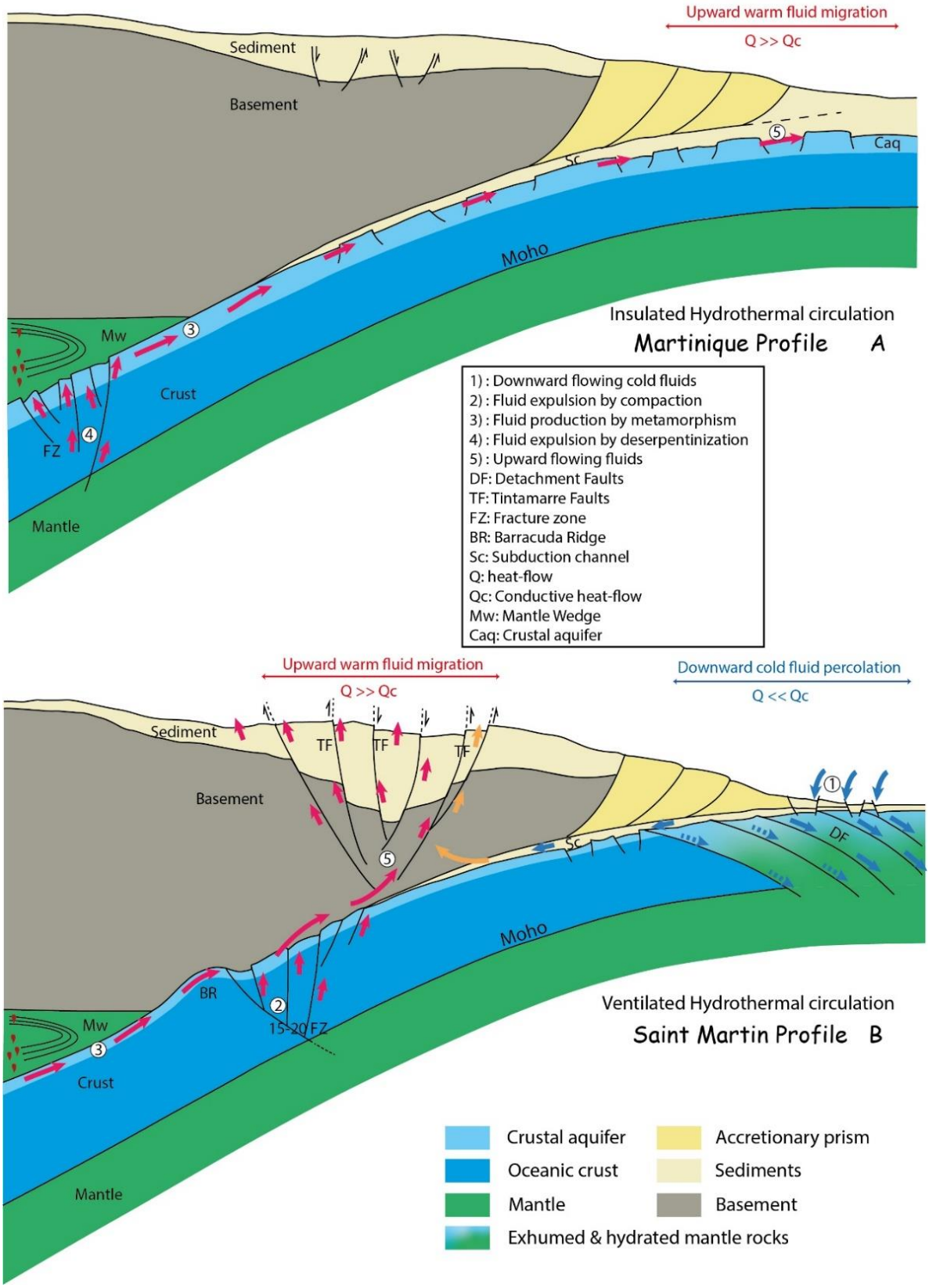

Figure 6: Interpretative sketches of the fluid circulation in the subduction for (A) an insulated hydrothermal system in the Central Lesser Antilles, offshore of Martinique and (B) a ventilated hydrothermal system in the Northern Lesser Antilles, offshore of Saint Martin. The structures are based on MCS profiles and Wide Angle interpretations of (Laigle et al., 2013b, Kopp et al., 2011) for the Martinique profile, and (Boucard et al., 2021, Marcaillou et al., 2021, Laurencin et al., 2018) for the Saint Martin profile (See section 2 for details).

5.1 Central Lesser Antilles, offshore of Martinique

Along the Martinique profile, the heat flow is significantly higher than the conductive value in the trench, decreasing regularly landward beneath the forearc. This behavior is typical of shallow hydrothermal warming related to insulated circulation, as described for instance in Nankai (Spinelli & Wang, 2008, Harris et al., 2017). In the Central Lesser Antilles, Boron isotope ratio indicates excess dehydration, i.e. high rate of water released from the slab, at great depth beneath the volcanic arc (Cooper et al., 2020). These authors thus confirm previous geophysical studies, which highlighted the strong hydration of this subduction segment (Schlaphorst et al., 2016, Paulatto et al., 2017). They indicate that the subduction of numerous deep large-scale oceanic transform fault zones and potentially exhumed mantle rocks related to the slow-spreading Mid-Atlantic Ridge have the potential to supply substantial volumes of fluid to the subduction. We propose that warm fluids, released at shallow depths by sediment compaction and at greater depths by metamorphic dehydration and/or deserpentinization of exhumed mantle rocks along major fracture zones (e.g. Marathon F.Z.), collected within the oceanic basement aquifer and the interplate fault zone, migrate updip along the subduction interface and the shallow crustal aquifer toward the trench, as exemplified in Chile by Moreno et al. (2014) and in Nankai by Spinelli & Wang, (2008). The 2-to-3-km thick poorly-faulted sedimentary trench fill to the South of the Barracuda Ridge, impedes cold seawater downward percolation into the trench, insulating the downgoing oceanic plate. As a result, fluids updip migration warms up the subduction interface beneath the shallow portion of the accretionary prism, the deformation front and the trench, increasing the heat-flow at the seafloor (Figure 6A).

5.2 Northern Lesser Antilles, offshore of Saint Martin

Along the Saint Martin profile, the measured heat flow is significantly lower than the conductive value in the trench and at the accretionary wedge. This behavior is typical in the presence of shallow hydrothermal cooling and ventilated circulation, as described for instance in Costa-Rica (Harris & Wang, 2002, Harris et al., 2010). In the trench, the subducting oceanic basement within the Jacksonville patch consists of exhumed and hydrated mantle rocks deeply and pervasively fractured by widespread detachment faults overlain with a fractured <500-m-thin sedimentary layers (Marcaillou et al., 2021). These detachment faults, likely reactivated by plate bending, and the thin fractured sedimentary layers favor downward cold seawater percolation and hydrothermal cooling in the trench. Outside the Jacksonville patch, within the oceanic domain, a second heat-flow measurement (55mW/m²) is consistent with an expected conductive heat-flow value. However, this region shows no evidence of highly faulted sediment and oceanic basement as observed in the patch (Marcaillou et al., 2021). Thus, it is likely that hydrothermal cooling maybe restricted to the extent of the Jacksonville patch in the oceanic domain. However, this is based only on the 2 heat-flow values acquired inside and outside of the patch respectively. In the forearc, the Tintamarre Fault deeply fractures the basement, while the 15-20 Fracture Zone deeply fractures the subducting oceanic plate at greater depth beneath the forearc. The

slab dehydration at depth, by sediment compaction, metamorphic reactions and deserpentinization of basement and/or mantle rocks probably releases large amount of fluids into the interplate fault damaged zone. We propose that the >100-km-long and 60-km-wide Tintamarre Fault Zone associated to intense basal erosion (Boucard et al., 2021) offers efficient pathways for fluid upward migration up to the seafloor where they create numerous possible pockmarks (Klingelhoefer et al., 2018). As a result, downward percolation of cold seawater through reactivated detachment faults in the trench, and warm fluid upward migration through major fault zones in the forearc are consistent with heat-flow measurements respectively lower and higher than conductive value in this ventilated hydrothermal system (Figure 6B).

6 Thermal structure and potential seismogenesis

The thermal structures for the Saint Martin and Martinique profile models, with and without heat advection, show small variations in the location of the 100, 150, 350 and 450°C isotherms often interpreted to be associated with the updip and downdip limit of seismogenic zones when located at shallower depth than hydrated mantle wedge (e.g. Hyndman et al., 1995) (

(A) Martinique model	**Conductive Model**		**Insulated Model**	
Isotherm	Distance from deformation front (km)	Depth (km)	Distance from deformation front (km)	Depth (km)
100°C	80	12	75	10
150°C	140	22	124	20
350°C	220	60	220	60
450°C	250	85	250	85
(B) Saint Martin model	**Conductive Model**		**Insulated Model**	
Isotherm	Distance from deformation front (km)	Depth (km)	Distance from deformation front (km)	Depth (km)
100°C	50	12	60	15
150°C	100	23	110	25
350°C	180	62	180	65
450°C	205	80	205	80

Table 1 and Figure 7).

When comparing the effect of advection vs conduction, offshore of Martinique, fluid updip migration warms up a shallow section of the interplate contact, from 190 km to the trench, shifting the 150°C isotherms seaward by 15 km. In contrast, this heat advection has no effect on the thermal structure of the deepest part of the interplate contact, which is mostly controlled by the mantle wedge. Along the Saint Martin profile, cold fluid downward percolation in the Jacksonville Patch cools down the temperature of the frontal segment of the interplate contact and this cooling effect rapidly decreases landward. As a result, the 100 and 150°C isotherms are shifted by 10 km by this hydrothermal cooling, which has no impact on the location of the 350 and 450°C isotherms. The moderate effect of this

hydrothermal circulation onto the thermal structure is likely related to the old age of the oceanic plate and the slow convergence rate. The age and convergence rate of the oceanic plate in the LA typically generate cold subduction zone and thus reduce the influence of hydrothermal circulation onto the thermal structure.

What is noteworthy are the significant distances from the trench of the 150°C and 350°C temperatures on the interplate fault : they are both located beneath the inner forearc for the Saint Martin profile and beneath the outer forearc for the Martinique profile. The distance between the 150°C and 350°C, often referred to as the minimum width of the thermally defined seismogenic zone, varies from 80 to 94 km for the Martinique profile, and from 80 to 72 km for the Saint Martin profile from the conductive to the advective models.

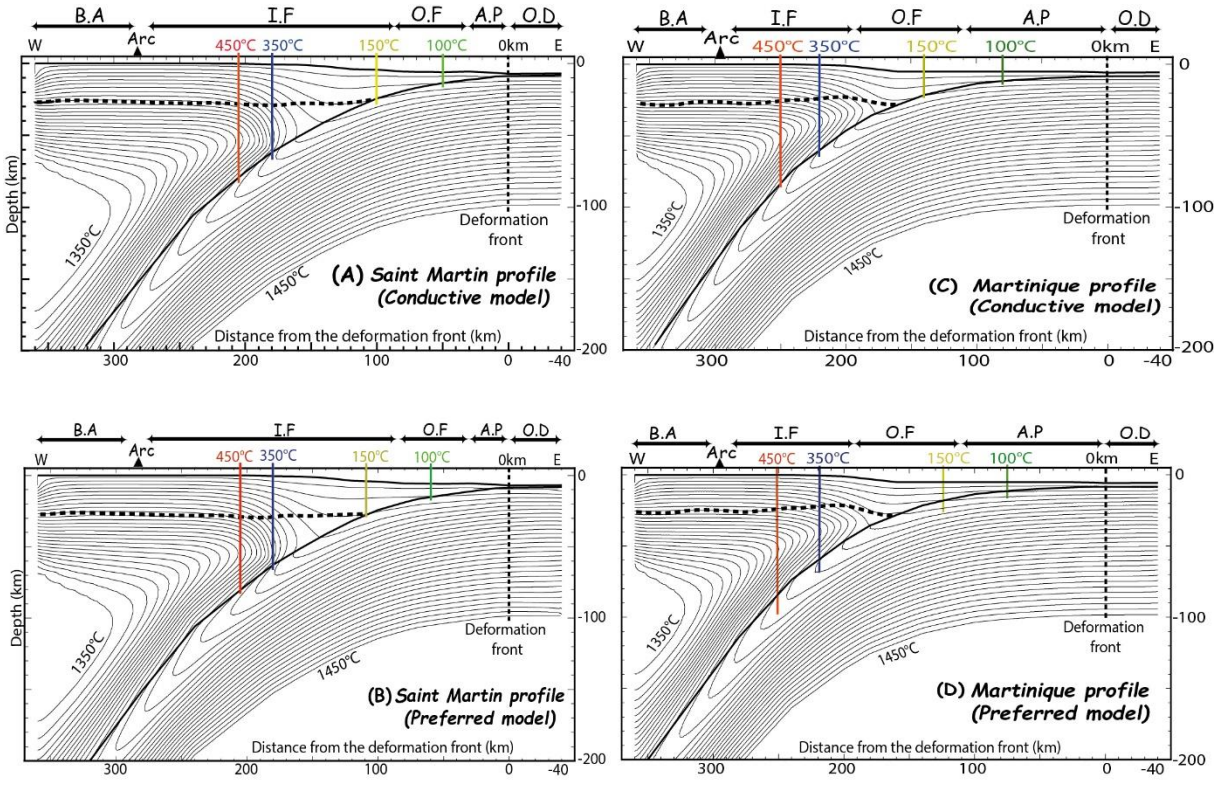

Figure 7: Thermal structure of the Lesser Antilles Margin at the latitude of Saint Martin (A, B) and Martinique (C, D) predicted by the conductive models and the advective models (preferred models). The location of the 100, 150, 350 and 450°C isotherms are marked with vertical lines.

(A) Martinique model	**Conductive Model**		**Insulated Model**	
Isotherm	Distance from deformation front (km)	Depth (km)	Distance from deformation front (km)	Depth (km)
100°C	80	12	75	10
150°C	140	22	124	20
350°C	220	60	220	60
450°C	250	85	250	85

(B) Saint Martin model	Conductive Model		Insulated Model	
Isotherm	Distance from deformation front (km)	Depth (km)	Distance from deformation front (km)	Depth (km)
100°C	50	12	60	15
150°C	100	23	110	25
350°C	180	62	180	65
450°C	205	80	205	80

Table 1: Calculated depth and distance from the deformation front for isotherms 100°C, 150°C, 350°C and 450°C for the Martinique (A) and Saint Martin (B) models. These isotherms are commonly associated with the updip and downdip limits for the thermally-defined seismogenic zone.

Along the Martinique profile, temperatures of 150°C and 350°C reach depths of 20 km and 60 km respectively on the interplate fault. The forearc Moho located at a shallower depth (28 km) than 350°C would thus become the downdip limit of the potential seismogenic portion (Hyndman et al., 1997), with a sharp reduction of the width to 36 km. On the Saint Martin Profile, a greater depth of 25 km for the 150°C marking the updip limit, and a shallower moho (25 km) appear to further reduce the potential width of the seismogenic portion, making it potentially almost non-existent. In case of subducting exhumed mantle patches within the slab's crust outcropping along the plate interface, seismogenic width will be even more reduced due to their expected serpentinization at those low temperatures. However, we can still not quantify the degree of serpentinization of these mantle materials (wedge and slab's crust) along the interplate contact, and these new measurements and models of thermal structure provide up-to-date estimations of temperatures along the megathrust fault. Moreover, up to Mw ~5 flat-thrust events have been recorded at the depth of 40-45 km (Laigle et al., 2013), and up to 51 km (Bie et al., 2019) in the Central Lesser Antilles, offshore Martinique. These events highlight a deep seismogenic zone which appears to extend (or resume) beyond the intersection between the forearc moho and the interplate, but raises question as to the nature of the subducting crust and/or the forearc mantle materials.

7 Relationship between temperature, fluids, and seismicity

We investigate the relationship between the thermal structure of the margin, fluid release, and the location of intraslab, supraslab, and interplate seismicity (Figure 8). We put a particular emphasis on the Martinique profile (Figure 8A) where 5.5-years-long OBS deployments provide us with numerous and accurately relocated earthquakes (Laigle et al., 2013a). In contrast, the seismicity in the vicinity of the Saint Martin profile is sparse and poorly located (Figure 8B).

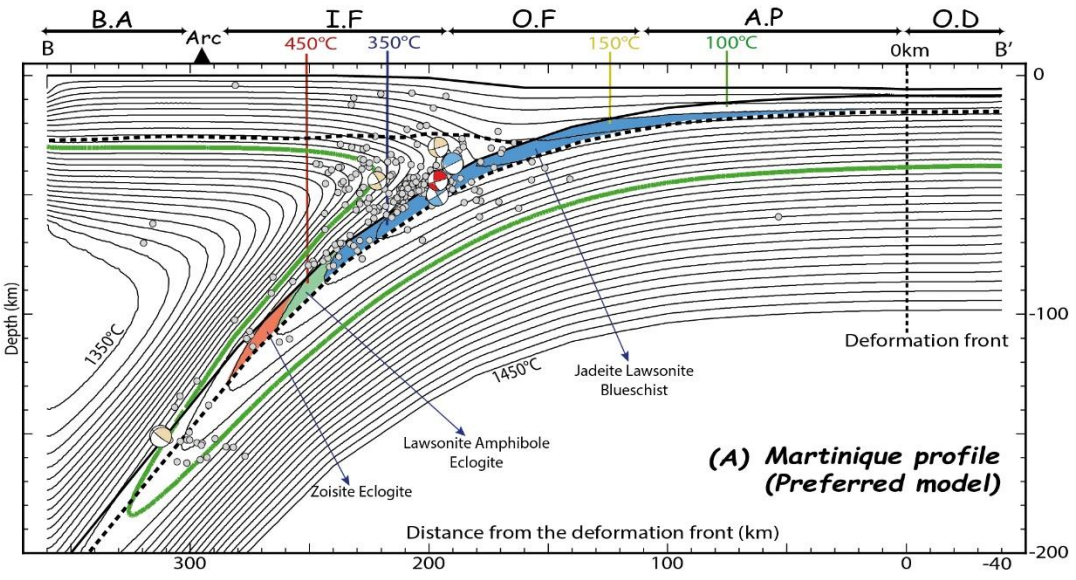

435

436

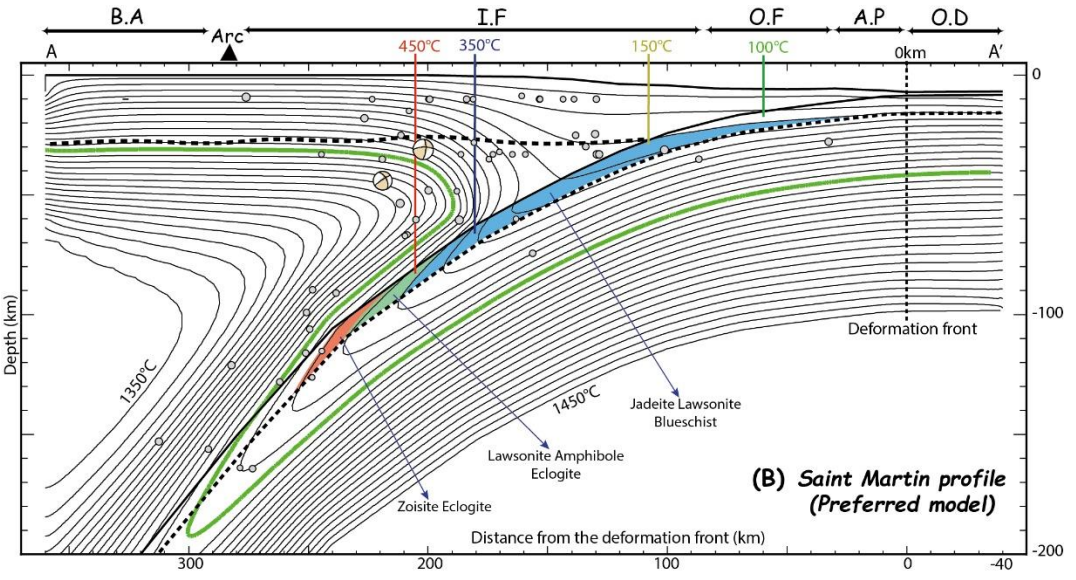

437

438 *Figure 8: Thermal structure of the LASZ with cross-sections of the hypocenters for earthquakes located*
439 *within 25 km on each side of the Martinique (A) and Saint Martin (B) profiles (see figure 2). The gray circles are*
440 *relocated earthquakes from OBS deployment (Laigle et al., 2013a) for the Martinique profile, and earthquakes*
441 *from USGS catalogue for Saint Martin profile. The blue focal mechanisms are thrust faults, and the red is a*
442 *relocated flat thrust event, while the yellow represents other focal mechanism from CMT catalogue. The black*
443 *thick line represent the top of the subducting slab, while the black dotted lines represent the Moho. The green*
444 *contour line marks the 600 °C isotherm usually considered as an averaged temperature for antigorite dehydration.*

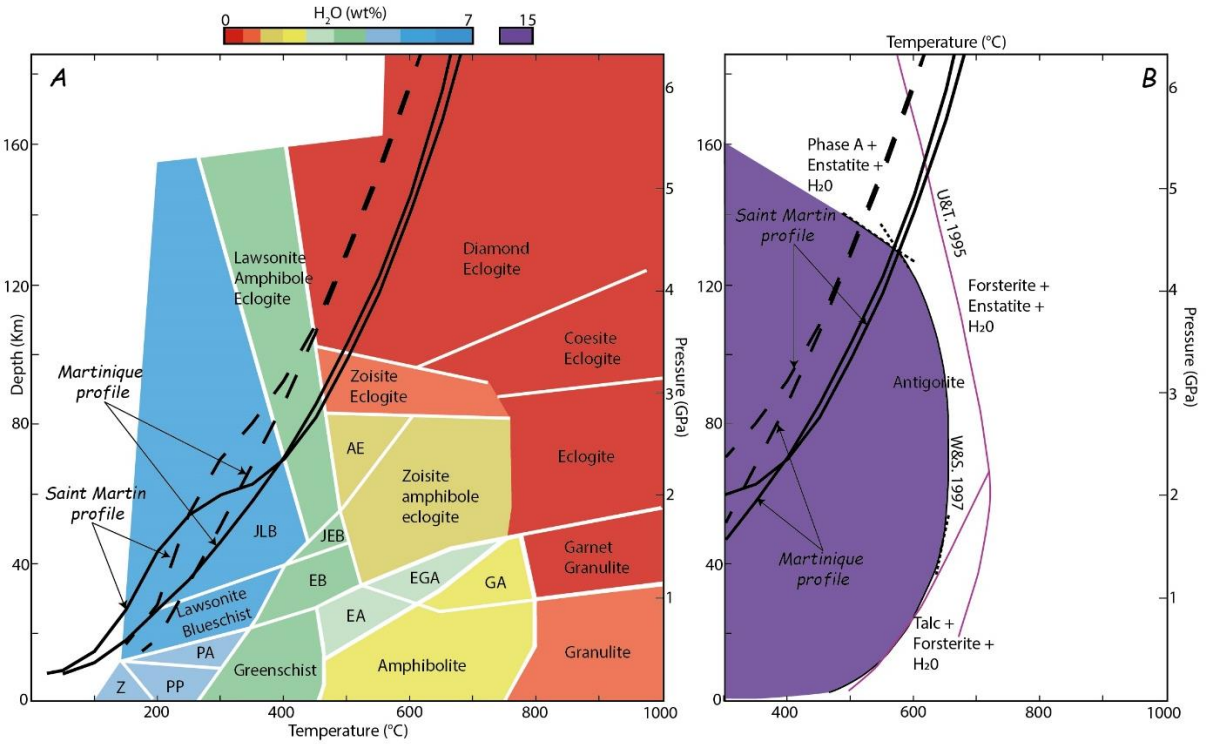

Figure 9: Phase diagram and maximum H_2O content for (A) metamorphosed MORB modified from Hacker, et al., (2003) and (B) hydrated mantle modified from (Wunder & Schreyer, 1997 and Ulmer & Trommsdorff, 1995), showing the Pressure-Temperature (PT) path for the slab tops (thick black lines), and moho (dash lines) offshore of Martinique and Saint Martin in the LASZ. (Z – Zeolite, PP – Prehnite pumpellyite, PA – Prehnite actinolite, JLB – Jadeite lawsonite blueschist, EB – Epidote blueschist, EA – Epidote amphibolite, JEB – Jadeite epidote blueschist, AE – Amphibole eclogite, EGA – Epidote garnet amphibolite, GA – Garnet amphibolite).

7.1 Intraslab seismicity

At depth in subduction zones, the location of intraslab seismicity is mainly controlled by the combined influence of pressure, temperature, slab bending stresses, and fluid release related to dehydration reactions, in particular, crust eclogitisation and mantle deserpentinization (Kirby et al., 1996; Hacker et al., 2003; Ferrand, 2019). Intraslab seismicity in the LASZ is distributed both within the crust and the mantle of the slab. At the LASZ, numerous fracture zones and detachment faults deeply incise the basement of the incoming oceanic plate, down to the mantle, likely favoring deep hydration and serpentinization of mantle rocks before the trench (Cooper et al., 2020; Marcaillou et al., 2021). These hydrated rocks are more stable at shallow depths and transport volatiles to dehydrate at greater depths during deserpentinization reaction at temperatures greater than 450°C (Ulmer & Trommsdorff, 1995 and Van Keken et al., 2011; Ferrand, 2019; Bie et al., 2022). Since the composition of the subducting oceanic crust of the slow-spreading mid-Atlantic ridge can vary from mid-oceanic basalt up to serpentinized exhumed mantle, we report the slab's top and moho on a phase diagram for metamorphosed mid-oceanic ridge basalt (MORB) (e.g. Hacker, et al., 2003) and for hydrated mantle materials (e.g. Wunder & Schreyer, 1997; Ulmer & Trommsdorff, 1995) (Figure 9A & B). We also report on the thermal structure and seimicity cross-section (Figure 8A) the main metamorphic facies of

the MORB phase diagram, as well as the 600 °C isotherm which could be used as a proxy of the maximum temperature for antigorite stability (650°C).

Slab's intracrustal seismicity in the LASZ is distributed between 35 and 165 km depth, which corresponds to calculated temperature's range of 240-625°C (Figure 8A). According to the *PT* path of the slab's top and moho, slab's intracrustal seismicity at 70-80 km depth at 400-450°C could result from dehydration reaction at the Blueschist-Eclogite transition. This depth is consistent with the downdip extent of the low-Vp anomaly in the slab crust and the transition towards higher Vp interpreted to be the result of crustal eclogitization (Paulatto et al., 2017). Fluids generated by dehydration reactions could migrate upward into the mantle wedge and updip through the slab, driven by gradients in tectonic stresses related to slab bending/unbending and densification (Faccenda et al., 2012; Paulatto et al., 2017), induce hydrofracturing, and trigger earthquakes within the shallow slab crust at 35-70 km depth. The oceanic crustal portions made of exhumed serpentinized peridotites is expected to dehydrate at depths >130 km above 550°C, and also be responsible for fluids upward migration and associated seismicity by dehydration embrittlement at these depths.

Within the slab mantle, the seismicity is aggregated in two main zones within a ~25-km-thick band beneath the slab top, at 35-80 km and 140–165 km depths, which correspond to calculated intraslab temperature's range of 250-450°C and 550-800°C respectively (Figure 8A). According to *PT* path of the slab's moho reported on the hydrated mantle phase diagram (Figure 9B), antigorite is expected to be unstable from 140 km at 520°C and up to ~620°C within the slab mantle along the depth of 160 km. Thus, we propose that the deeper intraslab seismicity zone located at 140–165 km depth, within the antigorite destabilization zone, is related to dehydration of serpentinized peridotite. This is consistent with elevated Vp/Vs ratio observed at similar depth which is interpreted to correspond to peak water release (Bie et al., 2022). For the shallower active zone within the slab mantle at 35-80 km depth, the deepest events below the slab top close to the isotherms of >450-520°C could be associated to antigorite destabilization process-related temperatures as proposed by Laigle et al., (2013a). The shallower events within the 20 km thick mantle band below the slab top may be linked to other processes similar to the reactivated faults of this slow-spreading oceanic lithosphere. The origin of the seismic activity located in the footwall of the deep-rooted detachments faults at the Mid-Atlantic ridge down to ~10 km depth (e.g. Parnell-Turner et al., 2017) is not yet really understood. However, their seismogenic potential might persist even at those depths of 50 km, thanks to the still preserved thermal structure of the lithospheric mantle.

7.2 Supraslab seismicity

Supraslab earthquakes, offshore of Martinique are aggregated in a cluster located at 30-60 km depth in the mantle wedge, and extending up to 80 km arcward of the contact between the interplate and the upper plate moho (Figure 1Figure 8A). The seismicity occurring above the slab at depths greater than 100 km may be interplate or slab crust/mantle events, and could be related to uncertainties of seismicity

location/ or slab geometry. The supraslab seismicity zone is distributed over isotherms between 200°C and 800°C. At temperature below 450°C, antigorite is expected to be stable, and mantle rocks to undergo serpentinization in the presence of fluid. Existing hypothesis for supraslab seismicity in the LASZ suggests heterogeneous mantle wedge and upward fluid migration (Laigle et al., 2013a; Paulatto et al., 2017). Our predicted temperature and depth of crustal eclogitization and fluid production at 70-80 km supports this hypothesis for the earthquakes occurring at least ~50 km arcward of the mantle wedge corner, at temperatures lower than 500°C. Beyond the 50 km distance, and between 500-800°C, we propose that supraslab seismicity in this subduction zone could be related to dehydration embrittlement due to deserpentinization reaction in the serpentinized mantle wedge, as invoked beneath northeast New Zealand (e.g. Davey & Ristau, 2011).

7.3 Interplate seismicity

Interplate seismicity is located at depth greater than 25 km, and distance greater than 160 km from the deformation front (Figure 8A), and includes deep moderate size flat-thrust earthquakes between 40-50 km depth and 190-200 km distance from the deformation front. This seismicity corresponds to calculated temperatures ranging from 200°C and 450°C at the slab top, while the upper-plate Moho intersects the subduction interface at ~28 km depth and temperature of ~210°C. The interplate seismogenic zone thus extends downdip of the upper-plate Moho, consistently with other cold subduction zones, e.g. Tohoku, where flat-thrust earthquakes are observed at similar depth in the Mantle (Uchida & Matsuzawa, 2011). Thermal models predict a cold forearc mantle above the location of the Mw 5 flat-thrust event (Figure 8A), and downdip slab dehydration, with updip fluid migration into the mantle wedge, favourable for serpentinization reaction to occur. This result suggests that dry peridotite in the mantle is unlikely, rather, tilts towards existing hypothesis of chemical heterogeneity of the mantle corner (Laigle et al., 2013a) as mechanism for this “deep flat-thrust” earthquakes. The interplate contact beneath the forearc, from the trench to 110-125 km distance westward (Table 1), corresponds to temperatures lower than 150°C, frequently considered as poorly, or conditionally favorable to stick-slip behavior. Hence, temperatures lower than 100°C below the accretionary prism make seismic rupture up to the trench very unlikely. Thus, the thermal models highlight a deep “thermally-defined seismogenic zone” (i.e. 150° - 350°C temperature range), typical of cold subduction zones, associated with intense fluid circulation from the subduction depth to the trench.

These features shed light on the mechanical conditions and the sliding behavior along the interplate contact at the Lesser Antilles. Geodetic modelling predict very low interplate coupling (van Rijsingen et al., 2021) consistent with scarce interplate thrust earthquakes mostly aggregated in two local clusters (Hayes et al., 2013) (see details in §2.2). Intense fluid circulation, as suggested by the thermal models, is able to increase the pore-fluid pressure, reducing the effective stress along the interplate contact (Moreno et al., 2014). A heterogeneous reduction of this effective stress may generate an interplate patchiness of contrasting frictional properties. Moreover, the rheology of low-temperature species of

serpentine minerals results in substantial weakening of serpentine-bearing faults and crustal rocks formed and altered at tectonically-dominated slow-spreading segments ridges (eg. Escartin et al., 1997). The ongoing subduction of tectonically-dominated oceanic patches, such as the Jacksonville patch identified at the trench (Marcaillou et al., 2021), may also favor this heterogeneity in interplate frictional properties. In subduction zones, the patchiness of contrasting frictional properties may impede large-scale zones of full interplate coupling (Hirauchi et al., 2010), instead favoring a mix of stable and unstable behaviors prone to triggering moderate-sized-Mw, slow-slip and/or very-low frequency earthquakes (Saffer & Wallace, 2015), and increasing time return of large co-seismic rupture.

Conclusion

Thermal models of the Lesser Antilles Subduction Zone, based on heat-flow data recorded during Antithesis 1 cruise (2013), show that fluid-driven heat advection strongly influences the heat transfer across the margin. Moreover, variations in heat-flow anomalies, compared to the regional conductive heat-flow, highlight the varying fluid flow pattern from ventilated to insulated circulation systems.

In the Central Lesser Antilles, offshore of Martinique, warm fluids released at depths in the subduction zone migrate updip along the subduction interface generating hydrothermal warming in the trench and at the margin front. The low level of fluid exchange with the water column is typical of insulated systems. Contrastingly, in the Northern Lesser Antilles, offshore of Saint Martin, downward percolation of cold fluids through crustal detachment faults in the trench triggers hydrothermal cooling at the margin front, while warm fluid upward migration through major fault zones in the forearc generates hydrothermal warming in the margin. These interpreted vigorous fluid exchanges with the water column are typical of ventilated systems.

Based on the model offshore Martinique, we show that intraslab, supraslab, and interplate seismicity distribution has a close relationship with temperature-related dehydration reactions at depth in the subduction. It is noteworthy that typical temperature and depth of eclogitisation and deserpentinisation reactions correspond to intraslab and supraslab seismicity clusters. Consistently with previous tectonic investigations, these thermal models confirm that the Northern Lesser Antilles is an end member subduction zone where the subduction of oceanic transform fault zones and oceanic patches partly made of exhumed and serpentinised mantle rocks deeply hydrate the subduction zone at depth. This “hyper-hydration” likely explains the very low interplate coupling and the scarce large co-seismic ruptures, possibly favoring alternate mode of sliding behavior, such as low velocity earthquakes, which are yet to be investigated.

CRediT authorship contribution statement

K.E. wrote the manuscript. **K.E.**, and **Y.B**. performed the thermal modelling supervised by **B.M.** and **M.L. B.M**, **F.K**, **J.-F.L.**, **F.R.**, **A.H.**, **T.P.**, **F.L.**, **M.P.**, **M.L.** and **B.H** were onboard RVs “l’Atalante” and “Pourquoi Pas?” during the ANTITHESIS cruise and acquired the heat-flow data. All authors discussed the scientific issues and commented on the manuscript.

Declaration of Competing Interest

The authors declare that they have no known competing financial interests or personal relationships that could have appeared to influence the work reported in this paper.

Acknowledgments

We thank the crew and the scientific party of the R/V "*Pourquoi Pas?*" for the heat-flow acquisition during marine surveys ANTITHESIS 1, leg 2. The thesis of Kingsley Ezenwaka is funded by the Petroleum Technology Development Fund (PTDF). We gratefully acknowledge Kelin Wang for providing the optimized version of the thermal modelling code.

References

Beardsmore, G. R., & Cull, J. P. (2010). Heat Flow. *Crustal Heat Flow*, 207–236. https://doi.org/10.1017/cbo9780511606021.007

Bernard, P., & Lambert, J. (1988). Subduction and seismic hazard in the northern Lesser Antilles: revision of the historical seismicity. *Bulletin - Seismological Society of America*, *78*(6), 1965–1983.

Bie, L., Hicks, S., Rietbrock, A., Goes, S., Collier, J., Rychert, C., Harmon, N., & Maunder, B. (2022). Imaging slab-transported fluids and their deep dehydration from seismic velocity tomography in the Lesser Antilles subduction zone. *Earth and Planetary Science Letters*, *586*, 117535. https://doi.org/10.1016/j.epsl.2022.117535

Bie, L., Rietbrock, A., Hicks, S., Allen, R., Blundy, J., Clouard, V., Collier, J., Davidson, J., Garth, T., Goes, S., Harmon, N., Henstock, T., Van Hunen, J., Kendall, M., Krüger, F., Lynch, L., Macpherson, C., Robertson, R., Rychert, K., … Wilson, M. (2019). Along-arc heterogeneity in local seismicity across the Lesser Antilles subduction zone from a dense ocean-bottom seismometer network. *Seismological Research Letters*, *91*(1), 237–247. https://doi.org/10.1785/0220190147

Boucard, M., Marcaillou, B., Lebrun, J. F., Laurencin, M., Klingelhoefer, F., Laigle, M., Lallemand, S., Schenini, L., Graindorge, D., Cornée, J. J., Münch, P., Philippon, M., & the, A. (2021). Paleogene V-Shaped Basins and Neogene Subsidence of the Northern Lesser Antilles Forearc. *Tectonics*, *40*(3), 1–18. https://doi.org/10.1029/2020TC006524

Braszus, B., Goes, S., Allen, R., Rietbrock, A., Collier, J., Harmon, N., Henstock, T., Hicks, S., Rychert, C. A., Maunder, B., van Hunen, J., Bie, L., Blundy, J., Cooper, G., Davy, R., Kendall, J. M., Macpherson, C., Wilkinson, J., & Wilson, M. (2021). Subduction history of the Caribbean from upper-mantle seismic imaging and plate reconstruction. *Nature Communications*, *12*(1). https://doi.org/10.1038/s41467-021-24413-0

Byerlee, J. (1993). Model for episodic flow of high-pressure water in fault zones before earthquakes. *Geology*, *21*(4), 303–306. https://doi.org/10.1130/0091-

7613(1993)021<0303:MFEFOH>2.3.CO;2

Calahorrano B., A., Sallarès, V., Collot, J. Y., Sage, F., & Ranero, C. R. (2008). Nonlinear variations of the physical properties along the southern Ecuador subduction channel: Results from depth-migrated seismic data. *Earth and Planetary Science Letters*, *267*(3–4), 453–467. https://doi.org/10.1016/j.epsl.2007.11.061

Cannat, M., Sauter, D., Mendel, V., Ruellan, E., Okino, K., Escartin, J., Combier, V., & Baala, M. (2006). Modes of seafloor generation at a melt-poor ultraslow-spreading ridge. *Geology*, *34*(7), 605–608. https://doi.org/10.1130/G22486.1

Carpentier, M., Chauvel, C., & Mattielli, N. (2008). Pb-Nd isotopic constraints on sedimentary input into the Lesser Antilles arc system. *Earth and Planetary Science Letters*, *272*(1–2), 199–211. https://doi.org/10.1016/j.epsl.2008.04.036

Cooper, G. F., Macpherson, C. G., Blundy, J. D., Maunder, B., Allen, R. W., Goes, S., Collier, J. S., Bie, L., Harmon, N., Hicks, S. P., Iveson, A. A., Prytulak, J., Rietbrock, A., Rychert, C. A., Davidson, J. P., Cooper, G. F., Macpherson, C. G., Blundy, J. D., Maunder, B., … Wilson, M. (2020). Variable water input controls evolution of the Lesser Antilles volcanic arc. *Nature*, *582*(7813), 525–529. https://doi.org/10.1038/s41586-020-2407-5

Davey, F. J., & Ristau, J. (2011). Fore-arc mantle wedge seismicity under northeast New Zealand. *Tectonophysics*, *509*(3–4), 272–279. https://doi.org/10.1016/j.tecto.2011.06.017

Davy, R. G., Collier, J. S., Henstock, T. J., Rietbrock, A., Goes, S., Blundy, J., Harmon, N., Rychert, C., Macpherson, C. G., Van Hunen, J., Kendall, M., Wilkinson, J., Davidson, J., Wilson, M., Cooper, G., Maunder, B., Bie, L., Hicks, S., Allen, R., … Labahn, E. (2020). Wide-Angle Seismic Imaging of Two Modes of Crustal Accretion in Mature Atlantic Ocean Crust. *Journal of Geophysical Research: Solid Earth*, *125*(6), 1–21. https://doi.org/10.1029/2019JB019100

De Min, L., Lebrun, J. F., Cornée, J. J., Münch, P., Léticée, J. L., Quillévéré, F., Melinte-Dobrinescu, M., Randrianasolo, A., Marcaillou, B., & Zami, F. (2015). Tectonic and sedimentary architecture of the Karukéra spur: A record of the Lesser Antilles fore-arc deformations since the Neogene. *Marine Geology*, *363*, 15–37. https://doi.org/10.1016/j.margeo.2015.02.007

DeMets, C., Jansma, P. E., Mattioli, G. S., Dixon, T. H., Farina, F., Bilham, R., Calais, E., & Mann, P. (2000). GPS geodetic constraints on Caribbean-North America Plate Motion. *Geophysical Research Letters*, *27*(3), 437–440. https://doi.org/10.1029/1999gl005436

Dziewonski, A. M., Chou, T. A., & Woodhouse, J. H. (1981). Determination of earthquake source parameters from waveform data for studies of global and regional seismicity. *Journal of Geophysical Research*, *86*(B4), 2825–2852. https://doi.org/10.1029/JB086iB04p02825

Ekström, G., Nettles, M., & Dziewoński, A. M. (2012). The global CMT project 2004-2010: Centroid-moment tensors for 13,017 earthquakes. *Physics of the Earth and Planetary Interiors*, *200–201*,

1–9. https://doi.org/10.1016/j.pepi.2012.04.002

Escartin, J., Hirth, J. G., & Evans, B. (1997). Effectts of serpentinization on the lithospheric strength and the style of normal faulting at slow-spreading ridges. *Earth and Planetary Science Letters*, *151*, 181–189.

Escartín, J., Smith, D. K., Cann, J., Schouten, H., Langmuir, C. H., & Escrig, S. (2008). Central role of detachment faults in accretion of slow-spreading oceanic lithosphere. *Nature*, *455*(7214), 790–794. https://doi.org/10.1038/nature07333

Evain, M., Galve, A., Charvis, P., Laigle, M., Kopp, H., Bécel, A., Weinzierl, W., Hirn, A., Flueh, E. R., & Gallart, J. (2013). Structure of the Lesser Antilles subduction forearc and backstop from 3D seismic refraction tomography. *Tectonophysics*, *603*, 55–67. https://doi.org/10.1016/j.tecto.2011.09.021

Faccenda, M., Gerya, T. V., Mancktelow, N. S., & Moresi, L. (2012). Fluid flow during slab unbending and dehydration: Implications for intermediate-depth seismicity, slab weakening and deep water recycling. *Geochemistry, Geophysics, Geosystems*, *13*(1). https://doi.org/10.1029/2011GC003860

Ferrand, T. P. (2019). Seismicity and mineral destabilizations in the subducting mantle up to 6 GPa, 200 km depth. *Lithos*, *334–335*, 205–230. https://doi.org/10.1016/j.lithos.2019.03.014

Feuillet, N., Beauducel, F., & Tapponnier, P. (2011). Tectonic context of moderate to large historical earthquakes in the Lesser Antilles and mechanical coupling with volcanoes. *Journal of Geophysical Research: Solid Earth*, *116*(10), 1–26. https://doi.org/10.1029/2011JB008443

Fisher, A. T., & Becker, K. (2000). Channelized fluid flow in oceanic crest reconciles heat-flow and permeability data. *Nature*, *403*(6765), 71–74. https://doi.org/10.1038/47463

Gutscher, M. A., Westbrook, G. K., Marcaillou, B., Graindorge, D., Gailler, A., Pichot, T., & Maury, R. C. (2013). How wide is the seismogenic zone of the Lesser Antilles forearc? *Bulletin de La Societe Geologique de France*, *184*(1–2), 47–59. https://doi.org/10.2113/gssgfbull.184.1-2.47

Hacker, B. R., Abers, G. A., & Peacock, S. M. (2003). Subduction factory 1. Theoretical mineralogy, densities, seismic wave speeds, and H 2 O contents . *Journal of Geophysical Research: Solid Earth*, *108*(B1), 1–26. https://doi.org/10.1029/2001jb001127

Hacker, B. R., Peacock, S. M., Abers, G. A., & Holloway, S. D. (2003). Subduction factory 2. Are intermediate-depth earthquakes in subducting slabs linked to metamorphic dehydration reactions? *Journal of Geophysical Research: Solid Earth*, *108*(B1). https://doi.org/10.1029/2001jb001129

Harris, R. N., Spinelli, G. A., & Fisher, A. T. (2017). Hydrothermal circulation and the thermal structure of shallow subduction zones. *Geosphere*, *13*(5), 1425–1444. https://doi.org/10.1130/GES01498.1

Harris, R. N., Spinelli, G. A., & Hutnak, M. (2020). Heat Flow Evidence for Hydrothermal Circulation in Oceanic Crust Offshore Grays Harbor, Washington. *Geochemistry, Geophysics, Geosystems*, *21*(6), 0–2. https://doi.org/10.1029/2019GC008879

Harris, R. N., Spinelli, G., Ranero, C. R., Grevemeyer, I., Villinger, H., & Barckhausen, U. (2010). Thermal regime of the Costa Rican convergent margin: 2. Thermal models of the shallow Middle America subduction zone offshore Costa Rica. *Geochemistry, Geophysics, Geosystems*, *11*(12), 1–22. https://doi.org/10.1029/2010GC003273

Harris, R. N., & Wang, K. (2002). Thermal models of the Middle America Trench at the Nicoya Peninsula, Costa Rica. *Geophysical Research Letters*, *29*(21), 6-1-6–4. https://doi.org/10.1029/2002GL015406

Hayes, G. P., McNamara, D. E., Seidman, L., & Roger, J. (2013). Quantifying potential earthquake and tsunami hazard in the Lesser Antilles subduction zone of the Caribbean region. *Geophysical Journal International*, *196*(1), 510–521. https://doi.org/10.1093/gji/ggt385

Hirauchi, K. I., Katayama, I., Uehara, S., Miyahara, M., & Takai, Y. (2010). Inhibition of subduction thrust earthquakes by low-temperature plastic flow in serpentine. *Earth and Planetary Science Letters*, *295*(3–4), 349–357. https://doi.org/10.1016/j.epsl.2010.04.007

Hough, S. E. (2013). Missing great earthquakes. *Journal of Geophysical Research: Solid Earth*, *118*(3), 1098–1108. https://doi.org/10.1002/jgrb.50083

Hutchison, I. (1985). The effects of sedimentation and compaction on oceanic heat flow. *Development*, *82*, 439–459.

Hyndman, R. D., & Wang, K. (1993). Thermal constraints on the zone of major thrust earthquake failure: the Cascadia Subduction Zone. *Journal of Geophysical Research*, *98*(B2), 2039–2060. https://doi.org/10.1029/92JB02279

Hyndman, R. D., Wang, K., & Yamano, M. (1995). Thermal constraints on the seismogenic portion of the southwestern Japan subduction thrust. *Journal of Geophysical Research*, *100*(15), 373–392.

Hyndman, R. D., Yamano, M., & Oleskevich, D. A. (1997). The seismogenic zone of subduction thrust faults. *Island Arc*, *6*(3), 244–260. https://doi.org/10.1111/j.1440-1738.1997.tb00175.x

Ildefonse, B., Blackman, D. K., John, B. E., Ohara, Y., Miller, D. J., MacLeod, C. J., Abe, N., Abratis, M., Andal, E. S., Andréani, M., Awaji, S., Beard, J. S., Brunelli, D., Charney, A. B., Christie, D. M., Delacour, A. G., Delius, H., Drouin, M., Einaudi, F., … Zhao, X. (2007). Oceanic core complexes and crustal accretion at slow-speading ridges. *Geology*, *35*(7), 623–626. https://doi.org/10.1130/G23531A.1

Kirby, S., Engdahl, E. R., & Denlinger, R. (1996). Intermediate-depth intraslab earthquakes and arc volcanism as physical expressions of crustal and uppermost mantle metamorphism in subducting slabs. *Geophysical Monograph Series*, *96*, 195–214. https://doi.org/10.1029/GM096p0195

Klingelhoefer, F., Marcaillou, B., Laurencin, M., Biari, Y., Laigle, M., Graindorge, D., Evain, M., Lebrun, J.-F., & Paulatto, M. (2018). Relation Between the Nature of the Subducting Plate, Heat Flow and Fluid Escape Structures at the Lesser Antilles Island arc. *American Geophysical Union*

Fall Meeting, Wahsington, DC, USA, T22B-04, 10–14.

Kodaira, S., Iidaka, T., Kato, A., Park, J. O., Iwasaki, T., & Kaneda, Y. (2004). High pore fluid pressure may cause silent slip in the Nankai Trough. *Science*, *304*(5675), 1295–1298. https://doi.org/10.1126/science.1096535

Kopp, H., Weinzierl, W., Becel, A., Charvis, P., Evain, M., Flueh, E. R., Gailler, A., Galve, A., Hirn, A., Kandilarov, A., Klaeschen, D., Laigle, M., Papenberg, C., Planert, L., & Roux, E. (2011). Deep structure of the central Lesser Antilles Island Arc: Relevance for the formation of continental crust. *Earth and Planetary Science Letters*, *304*(1–2), 121–134. https://doi.org/10.1016/j.epsl.2011.01.024

Kummer, T., & Spinelli, G. A. (2008). Hydrothermal circulation in subducting crust reduces subduction zone temperatures. *Geology*, *36*(1), 91–94. https://doi.org/10.1130/G24128A.1

Laigle, M., Hirn, A., Sapin, M., Bécel, A., Charvis, P., Flueh, E., Diaz, J., Lebrun, J. F., Gesret, A., Raffaele, R., Galvé, A., Evain, M., Ruiz, M., Kopp, H., Bayrakci, G., Weinzierl, W., Hello, Y., Lépine, J. C., Viodé, J. P., … Nicolich, R. (2013b). Seismic structure and activity of the north-central Lesser Antilles subduction zone from an integrated approach: Similarities with the Tohoku forearc. *Tectonophysics*, *603*, 1–20. https://doi.org/10.1016/j.tecto.2013.05.043

Laigle, M, Becel, A., de Voogd, B., Sachpazi, M., Bayrakci, G., Lebrun, J. F., & Evain, M. (2013a). Along-arc segmentation and interaction of subducting ridges with the Lesser Antilles Subduction forearc crust revealed by MCS imaging. *Tectonophysics*, *603*, 32–54. https://doi.org/10.1016/j.tecto.2013.05.028

Laurencin, M., Graindorge, D., Klingelhoefer, F., Marcaillou, B., & Evain, M. (2018). Influence of increasing convergence obliquity and shallow slab geometry onto tectonic deformation and seismogenic behavior along the Northern Lesser Antilles zone. *Earth and Planetary Science Letters*, *492*, 59–72. https://doi.org/10.1016/j.epsl.2018.03.048

Laurencin, M., Marcaillou, B., Graindorge, D., Klingelhoefer, F., Lallemand, S., Laigle, M., & Lebrun, J. F. (2017). The polyphased tectonic evolution of the Anegada Passage in the northern Lesser Antilles subduction zone. *Tectonics*, *36*(5), 945–961. https://doi.org/10.1002/2017TC004511

Laurencin, M., Marcaillou, B., Graindorge, D., Lebrun, J. F., Klingelhoefer, F., Boucard, M., Laigle, M., Lallemand, S., & Schenini, L. (2019). The Bunce Fault and Strain Partitioning in the Northern Lesser Antilles. *Geophysical Research Letters*, *46*(16), 9573–9582. https://doi.org/10.1029/2019GL083490

Lucazeau, F. (2019). Analysis and Mapping of an Updated Terrestrial Heat Flow Data Set. *Geochemistry, Geophysics, Geosystems*, *20*(8), 4001–4024. https://doi.org/10.1029/2019GC008389

Manga, M., Hornbach, M. J., Le Friant, A., Ishizuka, O., Stroncik, N., Adachi, T., Aljahdali, M.,

Boudon, G., Breitkreuz, C., Fraass, A., Fujinawa, A., Hatfield, R., Jutzeler, M., Kataoka, K., Lafuerza, S., Maeno, F., Martinez-Colon, M., McCanta, M., Morgan, S., … Wang, F. (2012). Heat flow in the Lesser Antilles island arc and adjacent back arc Grenada basin. *Geochemistry, Geophysics, Geosystems*, *13*(8), 1–19. https://doi.org/10.1029/2012GC004260

Marcaillou, B., & Klingelhoefer, F. (2013a). *ANTITHESIS-1-Leg1 Cruise, RV L'Atalante*. https://doi.org/doi:10.17600/13010070

Marcaillou, B., & Klingelhoefer, F. (2013b). *ANTITHESIS-1-Leg2 Cruise, RV Pourquoi Pas?* https://doi.org/doi:10.17600/13030100

Marcaillou, B., & Klingelhoefer, F. (2016). *ANTITHESIS-3 Cruise, RV Pourquoi Pas?* https://doi.org/doi:10.17600/16001700

Marcaillou, B., Klingelhoefer, F., Laurencin, M., Lebrun, J.-F., Laigle, M., Lallemand, S., Schenini, L., Gay, A., Boucard, M., Ezenwaka, K., & Graindorge, D. (2021). Pervasive detachment faults within the slow spreading oceanic crust at the poorly coupled Antilles subduction zone. *Communications Earth & Environment*, *2*(1). https://doi.org/10.1038/s43247-021-00269-6

Marcaillou, B., Spence, G., Wang, K., Collot, J. Y., & Ribodetti, A. (2008). Thermal segmentation along the N. Ecuador-S. Colombia margin (1-4°N): Prominent influence of sedimentation rate in the trench. *Earth and Planetary Science Letters*, *272*(1–2), 296–308. https://doi.org/10.1016/j.epsl.2008.04.049

Moore, J. C., & Saffer, D. (2001). Updip limit of the seismogenic zone beneath the accretionary prism of Southwest Japan: An effect of diagenetic to low-grade metamorphic processes and increasing effective stress. *Geology*, *29*(2), 183–186. https://doi.org/10.1130/0091-7613(2001)029<0183:ULOTSZ>2.0.CO;2

Moreno, M., Haberland, C., Oncken, O., Rietbrock, A., Angiboust, S., & Heidbach, O. (2014). Locking of the Chile subduction zone controlled by fluid pressure before the 2010 earthquake. *Nature Geoscience*, *7*(4), 292–296. https://doi.org/10.1038/ngeo2102

Müller, R. D., Zahirovic, S., Williams, S. E., Cannon, J., Seton, M., Bower, D. J., Tetley, M. G., Heine, C., Le Breton, E., Liu, S., Russell, S. H. J., Yang, T., Leonard, J., & Gurnis, M. (2019). A Global Plate Model Including Lithospheric Deformation Along Major Rifts and Orogens Since the Triassic. *Tectonics*, *38*(6), 1884–1907. https://doi.org/10.1029/2018TC005462

Parnell-Turner, R., Sohn, R. A., Peirce, C., Reston, T. J., MacLeod, C. J., Searle, R. C., & Simão, N. M. (2017). Oceanic detachment faults generate compression in extension. *Geology*, *45*(10), 923–926. https://doi.org/10.1130/G39232.1

Paulatto, M., Laigle, M., Galve, A., Charvis, P., Sapin, M., Bayrakci, G., Evain, M., & Kopp, H. (2017). Dehydration of subducting slow-spread oceanic lithosphere in the Lesser Antilles. *Nature Communications*, *8*, 240. https://doi.org/10.1038/ncomms15980

Pecher, I. A., Villinger, H., Kaul, N., Crutchley, G. J., Mountjoy, J. J., Huhn, K., Kukowski, N., Henrys, S. A., Rose, P. S., & Coffin, R. B. (2017). A Fluid Pulse on the Hikurangi Subduction Margin: Evidence From a Heat Flux Transect Across the Upper Limit of Gas Hydrate Stability. *Geophysical Research Letters*, *44*(24), 12,385-12,395. https://doi.org/10.1002/2017GL076368

Philibosian, B., Feuillet, N., Weil-Accardo, J., Jacques, E., Guihou, A., Mériaux, A. S., Anglade, A., Saurel, J. M., & Deroussi, S. (2022). 20th-century strain accumulation on the Lesser Antilles megathrust based on coral microatolls. *Earth and Planetary Science Letters*, *579*, 117343. https://doi.org/10.1016/j.epsl.2021.117343

Pichot, T., Patriat, M., Westbrook, G. K., Nalpas, T., Gutscher, M. A., Roest, W. R., Deville, E., Moulin, M., Aslanian, D., & Rabineau, M. (2012). The Cenozoic tectonostratigraphic evolution of the Barracuda Ridge and Tiburon Rise, at the western end of the North America-South America plate boundary zone. *Marine Geology*, *303–306*, 154–171. https://doi.org/10.1016/j.margeo.2012.02.001

Ranero, C. R., Morgan, J. P., McIntosh, K. D., & Reichert, C. (2003). Bending-related faulting and mantle serpentinization at the Middle America trench. *Nature*, *425*, 367–373.

Saffer, D. M., & Tobin, H. J. (2011). Hydrogeology and mechanics of subduction zone forearcs: Fluid flow and pore pressure. *Annual Review of Earth and Planetary Sciences*, *39*, 157–186. https://doi.org/10.1146/annurev-earth-040610-133408

Saffer, D. M., & Wallace, L. M. (2015). The frictional, hydrologic, metamorphic and thermal habitat of shallow slow earthquakes. *Nature Geoscience*, *8*(8), 594–600. https://doi.org/10.1038/ngeo2490

Schlaphorst, D., Kendall, J. M., Collier, J. S., Verdon, J. P., Blundy, J., Baptie, B., Latchman, J. L., Massin, F., & Bouin, M. P. (2016). Water, oceanic fracture zones and the lubrication of subducting plate boundaries-insights from seismicity. *Geophysical Journal International*, *204*(3), 1405–1420. https://doi.org/10.1093/gji/ggv509

Sibson, R. H. (2013). Stress switching in subduction forearcs: Implications for overpressure containment and strength cycling on megathrusts. *Tectonophysics*, *600*, 142–152. https://doi.org/10.1016/j.tecto.2013.02.035

Spinelli, G. A., & Wang, K. (2008). Effects of fluid circulation in subducting crust on Nankai margin seismogenic zone temperatures. *Geology*, *36*(11), 887–890. https://doi.org/10.1130/G25145A.1

Spinelli, G., Wada, I., Wang, K., He, J., Harris, R., & Underwood, M. (2018). Diagenetic, metamorphic, and hydrogeologic consequences of hydrothermal circulation in subducting crust. *Geosphere*, *14*(6), 2337–2354. https://doi.org/10.1130/GES01653.1

Stein, C. A., & Stein, S. (1994). Constraints on hydrothermal heat flux through the oceanic lithosphere from global heat flow. *Journal of Geophysical Research*, *99*(B2), 3081–3095. https://doi.org/10.1029/93JB02222

Szitkar, F., Dyment, J., Petersen, S., Bialas, J., Klischies, M., Graber, S., Klaeschen, D., Yeo, I., & Murton, B. J. (2019). Detachment tectonics at Mid-Atlantic Ridge 26°N. *Scientific Reports*, *9*(1), 0–8. https://doi.org/10.1038/s41598-019-47974-z

Tse, S. T., & Rice, J. R. (1986). Crustal earthquake instability in relation to the depth variation of frictional slip properties. *Journal of Geophysical Research*, *91*(B9), 9452. https://doi.org/10.1029/jb091ib09p09452

Tucholke, B. E., Lin, J., & Kleinrock, M. C. (1998). Megamullions and mullion structure defining oceanic metamorphic core complexes on the Mid-Atlantic Ridge. *Journal of Geophysical Research: Solid Earth*, *103*(5), 9857–9866. https://doi.org/10.1029/98jb00167

Uchida, N., & Matsuzawa, T. (2011). Coupling coefficient, hierarchical structure, and earthquake cycle for the source area of the 2011 off the Pacific coast of Tohoku earthquake inferred from small repeating earthquake data. *Earth, Planets and Space*, *63*(7), 675–679. https://doi.org/10.5047/eps.2011.07.006

Ulmer, P., & Trommsdorff, V. (1995). Serpentine stability to mantle depths and subduction-related magmatism. *Science*, *268*(5212), 858–861. https://doi.org/10.1126/science.268.5212.858

Van Keken, P. E., Hacker, B. R., Syracuse, E. M., & Abers, G. A. (2011). Subduction factory: 4. Depth-dependent flux of H2O from subducting slabs worldwide. *Journal of Geophysical Research: Solid Earth*, *116*(1). https://doi.org/10.1029/2010JB007922

van Rijsingen, E. M., Calais, E., Jolivet, R., de Chabalier, J.-B., Robertson, R., Ryan, G. A., & Symithe, S. (2022). Ongoing tectonic subsidence in the Lesser Antilles subduction zone. *Geophysical Journal International*, 319–326. https://doi.org/10.1093/gji/ggac192

van Rijsingen, E. M., Calais, E., Jolivet, R., de Chabalier, J. B., Jara, J., Symithe, S., Robertson, R., & Ryan, G. A. (2021). Inferring Interseismic Coupling Along the Lesser Antilles Arc: A Bayesian Approach. *Journal of Geophysical Research: Solid Earth*, *126*(2), 1–21. https://doi.org/10.1029/2020JB020677

Vrolijk, P. (1990). On the mechanical role of smectite in subduction zones. *Geology*, *18*(8), 703–707. https://doi.org/10.1130/0091-7613(1990)018<0703:OTMROS>2.3.CO;2

Wang, K., He, J., & Davis, E. E. (1997). Influence of basement topography on hydrothermal circulation in sediment-buried igneous oceanic crust. *Earth and Planetary Science Letters*, *146*(1–2), 151–164. https://doi.org/10.1016/s0012-821x(96)00213-0

Wang, K., Hyndman, R. D., & Yamano, M. (1995). Thermal regime of the Southwest Japan subduction zone: effects of age history of the subducting plate. *Tectonophysics*, *248*(1–2), 53–69. https://doi.org/10.1016/0040-1951(95)00028-L

White, R. S., Mckenzie, D., & Nions, K. O. (1992). Oceanic Crustal Thickness From Seismic Measurements and Rare Earth Element Inversions. *Journal of Geophysical Research*, *97*(B13),

856 19,683-19,715.
857 Wunder, B., & Schreyer, W. (1997). Antigorite: High-pressure stability in the system MgO-SiO2-H2O
858 (MSH). *Lithos*, *41*(1–3), 213–227. https://doi.org/10.1016/s0024-4937(97)82013-0
859